

# Wheel Odometry Model Calibration with Input Compensation by Optimal Control

Máté Fazekas, \* Péter Gáspár, \* Balázs Németh \*

\* *Institute for Computer Science and Control (SZTAKI), Eötvös  
Loránd Research Network (ELKH), Budapest, Hungary  
(e-mail: [mate.fazekas,peter.gaspar,balazs.nemeth]@sztaki.hu).*

---

**Abstract:** This paper presents an improved wheel odometry model calibration architecture to increase the accuracy and robustness of the motion estimation of vehicles. Wheel odometry is a robust and cost-effective method, but the accuracy of the estimation is limited by the knowledge of the parameter values. These can be estimated from GNSS and IMU measurements, but the calibration of the nonlinear odometry model in the presence of noise remains an open problem. Due to the nonlinearity, even with Gaussian-type measurement noise on the input wheel speeds, the calibration will be certainly biased. This paper presents an algorithm that takes advantage of the assumption that several measurements are available in a self-driving vehicle, and nowadays the increased computing capacity of computers allows more complex algorithms to be developed. With the proposed architecture, the bias of the model calibration can be reduced significantly through the application of the compensated input signals. The performance of the developed algorithm is demonstrated with detailed validation and test with a real vehicle.

*Keywords:* parameter estimation, optimal control, nonlinear system, least squares

---

## 1. INTRODUCTION

State estimation plays a critical role in self-driving software because trajectory planning and motion control are based on its results. The aim is to determine the motion signals, such as velocities and pose (position and orientation) as accurately as possible. Similarly, robustness and cost-efficiency are also important in the automotive industry, thus generally cost-effective automotive-grade types of sensors are applied. The disadvantages of the GNSS (Global Navigation Satellite System), IMU (Inertial Measurement Unit), or vision-based methods can be mitigated with the integration of wheel encoder measurements (Funk et al. (2017); Thrun and et al. (2006)). However, the model suffers from parameter uncertainty. Therefore, this paper focuses on the calibration of the odometry model, which is equivalent to the parameter identification of a nonlinear dynamic system. Generally, this type of optimization has not been solved yet, see e.g. (Schoukens and Ljung (2019)), and the problem is more difficult when the model calibration has to be performed with noisy signals.

The calibration problem of the wheel odometry model appears in the navigation task of small mobile robots first and has also become under investigation with the appearance of autonomous functions in the automotive industry. The related works operate with two different estimation methods. In the one, the parameter estimation is handled as a state filtering with the Augmented Kalman-filter

(Martinelli and Siegwart (2006); Brunner et al. (2017)). The process assumes zero dynamics for the parameters, thus it is a simple way to identify unknown values, but the convergence and observability are questionable (Martinelli and Siegwart (2006); Censi et al. (2013)), and a final stable value can not be obtained. The other method is to estimate the parameters as a regression problem, which due to the nonlinear model results in non-convex optimization. Its general solution is difficult, the methods such as (Censi et al. (2013); Seegmiller et al. (2013)) manage the nonlinear problem with double linearization or separation, however these only work with a simplified odometry model and almost perfect reference orientation measurements. In the case of a real-sized self-driving vehicle, these can not be presumed (Fazekas et al. (2020)).

When unknown parameters of a nonlinear model are identified, the key factor is the handling of the appearing noises. Linear system identification is a well-explored area (Ljung (1987)), but due to nonlinearity, there are new issues that do not appear at all in the linear case. Since the dynamics from the inputs to the outputs is not linear, the impact of the input noise can not be modeled with Gaussian distribution (which assumption is generally applied in the methods such as Kalman-filtering or least squares regression) on the measured output (Schoukens and Ljung (2019)). Thus, the model calibration will be biased certainly, even in the case of white noises on the measured input signals.

This distortion effect can be handled in two ways. The one is to apply specific requirements, such as unbiased estimation of the initial pose (Antonelli and et al. (2005)), measurement with expensive sensors (Lemmer et al. (2010)), or special pre-defined measurement scenarios (Jung et al.

---

\* The research was supported by the European Union within the framework of the National Laboratory for Autonomous Systems. (RRF-2.3.1-21-2022-00002). The paper was partially funded by the National Research, Development and Innovation Office (NKFIH) under OTKA Grant Agreement No. K 135512.

(2016)), etc. Only a few papers use the other way, which is to develop a specific algorithm that deals with the noises. In (Maye et al. (2016)), an undesirable behavior of the traditional observability analysis is examined. The proposed algorithm detects the case when due to the noises, the parameters seem to be observable, but in fact, they are not.

Our work addresses a different aspect of the distortion effect of the noises. No specific requirement is applied since a self-driving vehicle should re-calibrate itself from the signals of onboard sensors measured while general driving. For the parameter identification, the input wheel speed signals are also measured in addition to the output pose values. But due to the noise on these speed signals, input compensation, in other words, estimation of noise-free wheel speed signals is required. The main contribution is that the proposed calibration architecture includes input compensation besides the traditional parameter identification. The method operates with the Gauss-Newton nonlinear least squares technique and an optimal control task. The efficiency of the proposed algorithm is validated with experimental tests of a real-sized vehicle, which demonstrates that the mentioned issues of the noises are eliminated, and unbiased model calibration can be reached.

The remainder of the paper is organized as follows. In Section 2, the applied odometry model including dynamic wheel model is presented. The methods for nonlinear parameter identification, and the proposed improved calibration architecture with input compensation can be found in Section 3 and 4, respectively. The measurement scenarios used for the calibration are presented in Section 5. The validity of our approach is demonstrated via vehicle test experiments in Section 6, and finally, the paper is concluded in Section 7.

## 2. VEHICLE MODEL AND NOTATION

The navigation with wheel odometry is based on a model, where the state vector  $x_t$  contains the pose, the longitudinal and lateral positions of the center of gravity  $p_{x,t}, p_{y,t}$ , and the  $\psi_t$  orientation of the vehicle.

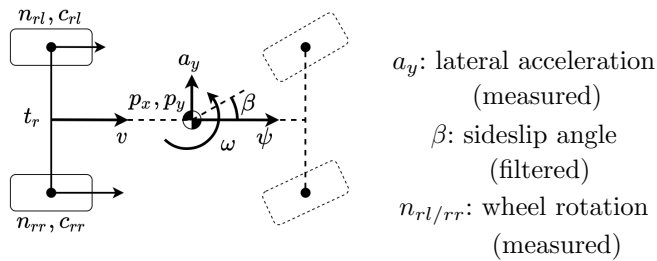


Fig. 1: Odometry model

The change of the pose is based on the longitudinal  $v_t$  and angular  $\omega_t$  velocities, thus the planar motion of the vehicle in  $t$  discrete time steps is calculated as,

$$\begin{bmatrix} p_{x,t+1} \\ p_{y,t+1} \\ \psi_{t+1} \end{bmatrix} = \begin{bmatrix} p_{x,t} + v_t \cdot t_s \cdot \cos(\psi_t + \frac{\omega_t}{2} + \beta_t) \\ p_{y,t} + v_t \cdot t_s \cdot \sin(\psi_t + \frac{\omega_t}{2} + \beta_t) \\ \psi_t + \omega_t \cdot t_s \end{bmatrix}, \quad (1)$$

where  $\beta_t$  is the sideslip angle filtered from the IMU and GNSS measurements. The velocities are computed utilizing the wheel rotations,

$$v_t = (n_{rl,t} \cdot c_{rl,t} + n_{rr,t} \cdot c_{rr,t})/2, \quad (2a)$$

$$\omega_t = (n_{rr,t} \cdot c_{rr,t} - n_{rl,t} \cdot c_{rl,t})/t_r, \quad (2b)$$

where  $t_s = 0.025$  s is the sampling time,  $c_{rl,t}, c_{rr,t}$  are the actual wheel circumferences, and  $t_r$  is the rear track width. The slight change of the wheel radius due to the effect of vertical dynamic is generally neglected, because the odometry-based localization is widely used in low-speed circumstances, e.g. automated parking. However, our method is developed for general driving, where the dynamics is significant (Fazekas et al. (2020)). Therefore, the slight change due to the vertical load transfer is considered,

$$c_{rl,t} = c_e + c_d/2 + d \cdot a_{y,t}, \quad (3a)$$

$$c_{rr,t} = c_e - c_d/2 - d \cdot a_{y,t}, \quad (3b)$$

where the  $c_e$  is the effective wheel circumference,  $c_d$  is the difference between the effective values,  $a_{y,t}$  is the lateral acceleration measured by the IMU, and the dynamic component  $d$  takes into account the effect of vertical dynamics.

In the calibration process, every state variable is measured, thus the system model is,

$$x_{t+1} = f(x_t, u_t, \theta), \quad x_t = [p_{x,t}, p_{y,t}, \psi_t]^T, \quad y_t = x_t, \quad (4a)$$

$$u_t = [n_{rl,t}, n_{rr,t}, \beta_t, a_{y,t}]^T, \quad \theta = [c_e, c_d, t_r, d], \quad (4b)$$

where  $f(\cdot)$  contains (1), and  $\theta$  is the parameter vector.

The nominal values of  $c_e$  and  $t_r$  can be found in the vehicle datasheet, but with these values, the position error of the model is already in the range of 10 m after a few hundred meters. The necessity of calibration is demonstrated with detailed motivation examples in our previous paper (Fazekas et al. (2021)), where a simplified calibration is presented.

Since in the paper a lot of signals are utilized with various forms, the following notations are introduced. The 'tilde' means the measured versions, e.g.  $\tilde{n}_{rl}$  and  $\tilde{n}_{rr}$  are measured with the wheel encoders. The signals of GNSS and IMU are filtered to form  $\tilde{y}$ , which will be named as measured pose. The 'hat' refers to estimated or computed versions, such as  $\hat{n}_{rl}$ ,  $\hat{n}_{rr}$  estimated wheel rotations,  $\hat{y}$  is the predicted output in the identification process, while  $\hat{x}$  is the computed nominal trajectory, and  $\hat{\theta}$  utilized as the estimated parameter vector. The measured lateral acceleration and filtered sideslip are utilized in the same version throughout the calibration, thus these are noted as  $a_y$  and  $\beta$  everywhere. The  $n_{rl}$  and  $n_{rr}$  wheel rotations will be mentioned several times with one symbol  $n_{rl/rr}$ .

## 3. NONLINEAR PARAMETER IDENTIFICATION

### 3.1 Parameter estimation of nonlinear dynamic models with Gauss-Newton method

Generally, the parameter estimation is formulated as a least squares (LS) optimization problem, to minimize the error of the  $\hat{y}_k(\theta)$  predictor of the model from the  $\tilde{y}_k$  output measurements, such as

$$\hat{\theta}_{opt} = \arg \min_{\theta} V_K(\theta) = \arg \min_{\theta} \sum_{k=1}^K \|\tilde{y}_k - \hat{y}_k(\theta)\|^2. \quad (5)$$

When the model is nonlinear in  $\theta$ , the optimization can only be solved with numerical search (Tangirala (2015)). We apply the Gauss-Newton (G-N) method that solves the nonlinear least squares problem with Taylor-approximation in the following way,

$$\hat{y}_k(\theta) \approx \hat{y}_k(\hat{\theta}_{i-1}) + \underbrace{\frac{\partial \hat{y}_k(\theta)}{\partial \theta}}_{j_k} \bigg|_{\hat{\theta}_{i-1}} \underbrace{(\hat{\theta} - \hat{\theta}_{i-1})}_{\Delta \theta}, \quad (6)$$

where due to the dynamic behavior of the predictor, the  $j_k$  jacobians are computed recursively. This results in a locally linear LS problem, such as

$$\hat{\Delta \theta}_{opt} = \arg \min_{\Delta \theta} \sum_{k=1}^K \|(\tilde{y}_k - \hat{y}_k(\hat{\theta}_{i-1})) - j_k \Delta \theta\|^2, \quad (7)$$

which can be solved with the LS solution in an iterative way,

$$\hat{\theta}_i = \hat{\theta}_{i-1} + (J^T W J)^{-1} J^T W R, \quad (8)$$

where the  $J := J(\hat{\theta}_{i-1})$ ,  $R := \tilde{Y} - \hat{Y}(\hat{\theta}_{i-1})$  matrices are formed from the  $j_k$  and  $(\tilde{y}_k - \hat{y}_k(\hat{\theta}_{i-1}))$  values, respectively.

A weight matrix  $W$  is also added to the basic solution. Since the model is linearized in the previous parameters, an initial guess for  $\theta$  is required, and when in last term  $(\tilde{Y} - \hat{Y}(\hat{\theta}_{i-1}))$  the integrated system model is computed with the previous parameters the states have to be initialized at the beginning of the estimation window.

In this identification method, the fundamental issues appear due to the noises on the  $\tilde{y}_k$  output and  $\tilde{u}_k$  input measurement signals. The noise on the  $\tilde{y}_k$  is less significant because it enters after the nonlinearity. The noise on the measured input must not be neglected, since its impact on the output can not be modeled with the Gaussian framework (Schoukens and Ljung (2019)). Because the methods like least squares or Kalman-filter apply this framework, the estimation would be biased. Therefore, our paper focuses on the compensation of input noise to guarantee unbiased model calibration.

### 3.2 Estimation in batch mode

The effect of the mentioned issues can be mitigated, if more measurement segments with length  $K$  are applied at once. In this batch mode, the matrices in the G-N method of the different segments are stacked into the following huge matrices,

$$J_B(\hat{\theta}_{B,i-1}) = \begin{bmatrix} J_1(\hat{\theta}_{B,i-1}) \\ \vdots \\ J_N(\hat{\theta}_{B,i-1}) \end{bmatrix}, R_B = \begin{bmatrix} \tilde{Y}_1 - \hat{Y}_1(\hat{\theta}_{B,i-1}) \\ \vdots \\ \tilde{Y}_N - \hat{Y}_N(\hat{\theta}_{B,i-1}) \end{bmatrix}, \quad (9)$$

where  $N$  denotes the batch size. The parameters can be identified in the same iterative way of (8) with the batch matrices. To avoid confusion, the G-N estimation that is performed on one individual segment (Section 3.1), will be noted as pure G-N method, while this as batch G-N.

In this batch case, the model fitting is performed to every segment simultaneously, which reduces the effect of the noises. The method is similar to a cross-validation technique inside the identification loop. However, it is important to note that the distortion effect of the input noise

is only reduced but not eliminated, thus the calibration remains biased.

## 4. CALIBRATION WITH INPUT COMPENSATION

### 4.1 Wheel rotation compensation with optimal control

In this paper, a new method is proposed to deal with the input noises to improve the model calibration. The main inputs of the odometry model are the wheel rotations, thus we focus on the compensation of the  $n_{rl/rr}$  wheel rotation signals only. The quantities are measured with the equipped encoder to the axle, but the signals are corrupted by slip and other noises. Since the errors do not pass through the system dynamics, these can not be determined with a disturbance estimator.

The noises of the measured  $\tilde{n}_{rl/rr}$  rotations can be compensated, if one form an estimation of the signals to determine the noise-free rotations. The idea is motivated by the well-known model predictive control strategy, where the optimal input sequence for the system to follow the reference trajectory can be determined by numerical optimization. Due to the nonlinearity of the odometry model, a Jacobian linearization of the model around a  $\hat{x}_k$  calculated nominal trajectory is performed,

$$\hat{A}_k = \frac{\partial f(\cdot)}{\partial x} \bigg|_{\hat{x}_k}, \hat{B}_k = \frac{\partial f(\cdot)}{\partial u} \bigg|_{\tilde{u}_k}, \hat{x}_{k+1} = f(\hat{x}_k, \tilde{u}_k, \theta), \quad (10a)$$

$$\hat{g}_k = f(\hat{x}_{k-1}, \tilde{u}_{k-1}, \theta) - (\hat{A}_{k-1} \hat{x}_{k-1} + \hat{B}_{k-1} \tilde{u}_{k-1}), \quad (10b)$$

and the following optimization task is formed,

$$\begin{aligned} \min_{n_{rl}, n_{rr}} \quad & \sum_{k=1}^K \|\tilde{y}_k - y_k(\theta)\|_Q^2 + \|\Delta n_{rl/rr,k}\|_R^2 \rightarrow \hat{n}_{rl/rr,k} \\ \text{s.t.} \quad & x_0 = \tilde{y}_0 \\ & x_k = \hat{A}_k x_{k-1} + \hat{B}_k u_{k-1} + \hat{g}_k \\ & \tilde{y}_k - [5, 5, 0.5] \leq x_k \leq \tilde{y}_k + [5, 5, 0.5] \\ & \tilde{n}_{rl/rr,k} \cdot 0.95 \leq n_{rl/rr,k} \leq \tilde{n}_{rl/rr,k} \cdot 1.05 \end{aligned} \quad (11)$$

which can be solved with quadratic programming (QP) techniques. The nominal trajectory  $\hat{x}_{k=1..K}$  is computed with the model (4) utilizing the measured  $\tilde{n}_{rl/rr,k}$  wheel rotations. The matrices  $Q$ , and  $R$  are positive definite weighting matrices of the trajectory tracking and the input changes, respectively. The initial state  $x_0$  is initialized with the corresponding  $\tilde{y}_k$  measured pose. The applied QP solver of Mathworks can handle lower and upper bounds (Mathworks (2021)). The states are bounded around the  $\tilde{y}_k$  measured values with limits of  $[5, 5, 0.5]$ . Since the estimated rotation signals are measured as well, a  $\pm 5\%$  limit around the  $\tilde{n}_{rl/rr,k}$  measured wheel rotations are applied. Utilizing these bounds the computation time is dramatically decreased, only a few iterations are enough for the convergence.

### 4.2 Calibration architecture

In the proposed calibration architecture, the batch G-N method (Section 3.2) is applied to identify the parameters, and the optimal control task (Section 4.1) is used to estimate the noise-free wheel rotation signals to improve

the calibration accuracy. These processes are integrated into a 3 steps calibration method, which can be found in detail in Figure 2. The process begins at the start, with preliminary filterings to calculate the required signals for the model calibration (Section 5).

Step 1: The novel idea in this paper is the input compensation, but the optimal control task (11) supposes known  $\theta$  parameter whose utilized value significantly affects the performance of the input estimation. To generate appropriate parameters for the  $n_{rl/rr}$  estimations, initial G-N identifications are performed in batch mode with  $N = 10$  segments resulting  $\hat{\theta}_{B,I}$  values.

Step 2: These are utilized as fixed parameters in the wheel rotation estimations. The  $n_{rl/rr}$  rotation inputs of every segment in the batch are compensated one by one. Since when the  $\hat{\theta}_{B,I}$  values are estimated in Step 1 the raw measured  $\tilde{n}_{rl/rr}$  rotations are used, the identified values are not accurate, and consequently neither are the estimated wheel rotations. Therefore, the estimated  $\hat{n}_{rl/rr}$  inputs of a segment are calculated as a mean of 5 optimal control estimations utilizing different  $\hat{\theta}_{B,I}$  parameters.

Step 3: Finally, the vehicle parameters are calibrated in batch mode, but now in every segment, the estimated  $\hat{n}_{rl/rr}$  inputs are utilized. Since the wheel rotation signals are compensated,  $N = 5$  batch size is sufficient to obtain proper  $\hat{\theta}_{B,F}$  identified values.

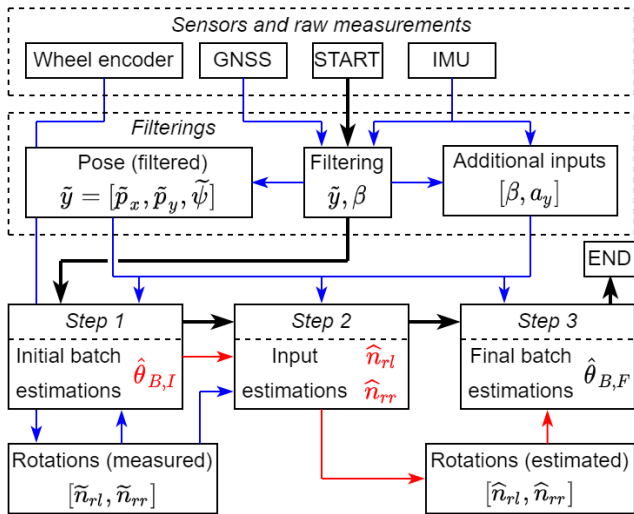


Fig. 2. Architecture of the proposed model calibration. Notations are: thick black arrow - process; blue arrow: addition signals to the calibration such as position, orientation, sideslip, acceleration; red arrow: estimated parameters and signals.

#### 4.3 Tuning of the method

In the Gauss-Newton parameter identification method, the  $W$  is introduced to equalize the lower value of orientation error in radians, than the position errors in meter. The experimental tuning results in the following setting,

$$w = [w_{p_x}, w_{p_y}, w_{\psi}] = [1, 1, 40^2],$$

$$W = [w, \dots, w]_{1 \times 3 K}, \quad W_B = [W, \dots, W]_{1 \times 3 K N},$$

to obtain proper vehicle model calibration. Due to the linearization in the G-N method, initial guess for the parameters are necessary. The nominal values ( $c_{e,nom} = 2 m$   $t_{r,nom} = 1.6 m$ ) from the vehicle's datasheet are applied, and the rests are set to zero.

$$\hat{\theta}_{B,0} = \theta_{nom} = [2, 0, 1.6, 0] \quad (13)$$

The iteration in the G-N method runs until the  $R$  residual is decreasing, or the maximum iteration  $i_{max} = 5$  is reached.

Since in our optimal control problem the estimated inputs are also measured and close to the true ones, a relatively high prediction horizon  $K = 650$  (15 s in time with 150 m average path length) can be applied. Despite, the computation is not high,  $i_{max} = 5$  iterations are sufficient due to the chosen bounds.

The main tuning parameters of the optimal control task are the  $Q$  and  $R$  weighting matrices, where only the diagonal elements are not zeros. Ensuring the trajectory tracking without high-frequency changes of the estimated inputs, the weights are chosen, such as

$$Q = \text{diag}([1, 1, 10]), \quad R = \text{diag}([1000, 1000]). \quad (14)$$

## 5. TEST VEHICLE AND MEASUREMENTS

The test vehicle is a Nissan Leaf electric car which is equipped with automotive-grade GNSS, compass, and IMU sensors, and from the vehicle CAN bus the wheel encoder signals are also saved. The sampling frequency is 40 Hz. The test track is a 24 km long route in suburb and city driving with normal driving conditions, the path can be found in Figure 3. The track contains various bends, two roundabouts, and lots of crossroads.

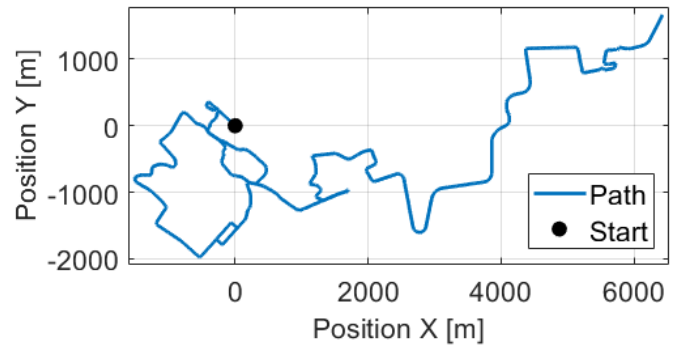


Fig. 3. Path of the used measurements scenario

The signals of the GNSS, compass, and IMU sensor are utilized for the model calibration. The pose can be measured directly with the first two, although these signals are assumed to be noisy but unbiased. In contrast, the pose computation from the acceleration and angular velocity measurements with the IMU is generally biased, but the noise is lower. The filtering problem is well-explored, the implemented method is similar to Caron et al. (2006) to obtain reference measurements ( $\tilde{y}_k$ ) for the estimation task. The sideslip is also estimated with an IMU-based method (Bewly et al. (2006)) in the bends, which are detected using the vehicle trajectory (Fazekas et al. (2021)).

The estimation is performed on smaller measurement parts, therefore, the 24 km long route is divided into

segments with  $K = 650$  measurement points and with step length  $2.5 \text{ s}$ . This results in 1025 segments with  $150 \text{ m}$  average lengths. Since the  $c_d, t_r$  and  $d$  parameters can be only observed properly with the yaw rate equations (2b), the 504 segments with higher absolute angular velocity than  $0.15 \text{ rad/s}$  are selected for the parameter estimation.

## 6. EXPERIMENTAL RESULTS

### 6.1 Validation error and reachable minimum

The true value of the  $\theta = [c_e, c_d, t_r, d]$  parameters are unknown, thus the model calibration can not be evaluated with the parameter estimation errors. Since the main goal of the calibration is to obtain a model which improves the motion estimation of a vehicle, the proposed method is validated with the position error of the calibrated models.

In order to avoid overfitting, the segments of the measured path are regenerated with different initial points and with  $300 \text{ m}$  average length. Furthermore, in the validation process, all of the parts are applied regardless of the angular velocity is lower than the limit. The validation error is the position one which is calculated such as,

$$E_{p,s} = \sum_{k=1}^K \sqrt{(\tilde{p}_{x,k} - p_{x,k}(\hat{\theta}))^2 + (\tilde{p}_{y,k} - p_{y,k}(\hat{\theta}))^2}, \quad (15a)$$

$$u_k = [\tilde{n}_{rl,k}, \tilde{n}_{rr,k}, \beta_k, a_{y,k}], \quad x_{k=0}(\hat{\theta}) = \tilde{y}_{k=0}, \quad (15b)$$

and the  $\bar{E}_p$  average of these segment errors is applied as a validation error to evaluate the method.

Take into account that the minimum validation error is not zero, because the states of the odometry model (4) at the beginning of the segment are initialized with the filter pose values, and the measured  $\tilde{n}_{rl/rr}$  rotations are utilized as inputs. The minimum error is  $2.40 \text{ m}$  determined with a genetic algorithm applying all of the validation segments.

### 6.2 Prior model calibrations (Step 1), examined batch

The proposed method is necessary because the batch version of the G-N method can not guarantee the bias-free parameter estimation. To illustrate this, 50 independent batches are formulated from the 504 selected segments with  $N = 10$  batch size. The resulted models are validated, the  $\bar{E}_p$  average errors can be found in Figure 4. The sorted

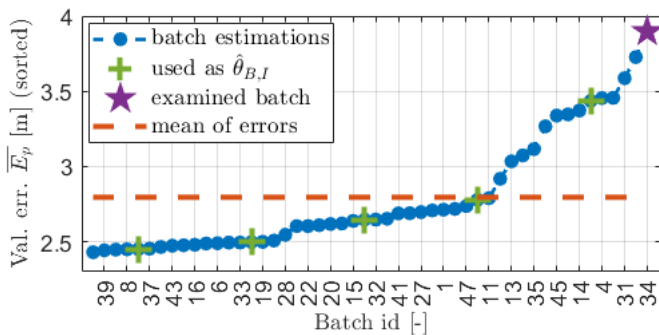


Fig. 4. Validation errors of the batch G-N estimations

error figure illustrates that it is possible to calibrate the odometry model with the batch G-N method since the best  $1/3$  of the calibrated models has a lower error than

$2.5 \text{ m}$ . On the other hand, the mean error of the worst  $1/3$  model is  $3.25 \text{ m}$ , even though 10 different segments are applied at once for the estimation. This demonstrates the necessity of noise compensation. The performance of the proposed method is illustrated in detail with the worst batch calibration (examined batch with id 34), to show the high impact of the wheel rotation noise compensation.

The input estimation in Step 2 could be accurate only if proper vehicle parameters are utilized in the model. In the first step of the calibration, the same G-N identification is performed, thus the 5  $\hat{\theta}_{B,I}$  vehicle parameter settings are chosen from the previously mentioned calibration. The models are selected with equal steps from the sorted list to ensure a realistic test of the proposed model (Figure 4).

The identified parameters of the selected  $\hat{\theta}_{B,I}$  settings, and the ones of the examined batch can be found in Figure 5. The standard deviations of the batch G-N calibrations are

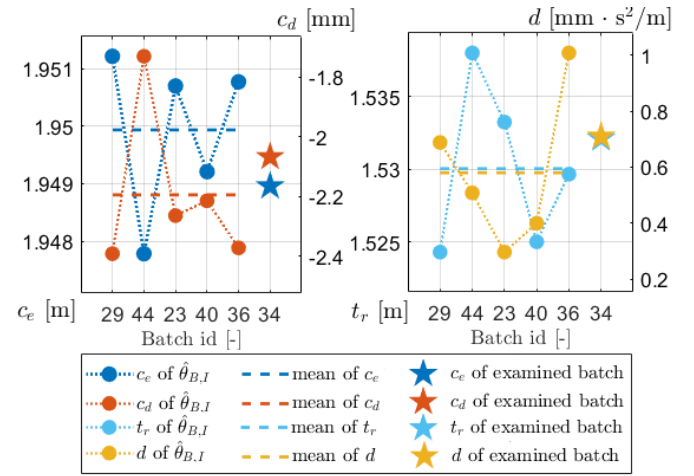


Fig. 5. Identified parameters of the 5  $\hat{\theta}_{B,I}$  G-N estimations (Step 1) and the examined batch

relatively low  $\sigma_{\theta_I} = [1.36, 0.20, 14.53, 0.27] \text{ mm}$ . However, one has seen in Figure 4 that the validation error of these models are in a range of  $2.45 - 3.90 \text{ m}$  with standard deviation of  $0.4 \text{ m}$ . Thus, the nonlinear wheel odometry model is highly sensitive to the parameters, e.g.  $0.5 \text{ mm}$  in the  $c_d$  circumference difference could result in  $0.8 \text{ m}$  higher validation error.

### 6.3 Input compensation on a given segment

First, the input compensation algorithm (Step 2) for segment 7 of the examined batch is illustrated. The input compensation algorithm (Section 4.1) is performed with the 5  $\hat{\theta}_{B,I}$  parameter setting. The mean of these are the  $\hat{n}_{rl}$  and  $\hat{n}_{rr}$  estimated wheel rotation signals (compensated inputs), which are illustrated in Figure 6 together with the measured ones. The estimated rotations are close to the measured ones, the main difference is the smoothness of the estimated signals, the absolute average of the relative error is below 1.2%.

Due to the nonlinear model, the impact of this small deviation should be analyzed. The pose errors of the odometry model (4) with the measured  $\tilde{n}_{rl/rr}$ , and compensated

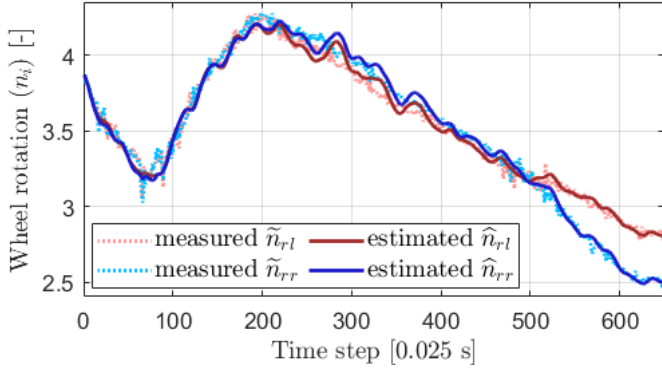


Fig. 6. The measured and estimated input signals

$\hat{n}_{rl/rr}$  inputs are  $[0.83 \text{ m}, 0.94^\circ]$  and  $[0.04 \text{ m}, 0.15^\circ]$ , respectively, which demonstrates that only a little noise in the wheel rotations could result in a significant deterministic error.

Since the main goal is the model calibration, the important question is the impact on the parameter identification. On this segment, estimations with the pure G-N method (Section 3.1) are performed utilizing the measured and estimated wheel rotations. The identified parameters and their validation errors can be found in the first two rows of Table 1. The high deviation of the identified parameters

Case	$c_e$	$c_d$	$t_r$	$d$	$\overline{E_p}$
Segment 7 with $\tilde{n}_{rl/rr}$	1.947	-0.70	1.654	-2.87	10.08
Segment 7 with $\hat{n}_{rl/rr}$	1.950	-2.08	1.527	0.73	2.51
Batch with $\tilde{n}_{rl/rr}$	1.950	-2.48	1.501	1.25	3.86
Batch with $\hat{n}_{rl/rr}$	1.950	-2.07	1.527	0.76	2.48

Table 1: Identified parameters with the measured ( $\tilde{n}_{rl/rr}$ ), and estimated ( $\hat{n}_{rl/rr}$ ) wheel rotations

is the consequence of the sensitivity to the input noise. Even though the estimated parameters with the raw measured  $\tilde{n}_{rl/rr}$  inputs are optimal in this segment, the 10  $m$  validation error shows that this is a totally wrong calibration. However, after the inputs are compensated, the odometry model can be calibrated properly with this single segment alone, which is illustrated with the 2.51  $m$  validation error.

#### 6.4 Calibration in batch mode with compensated inputs

In the previous section, the input estimation of one segment of the examined batch is presented, now the focus is on the model calibration with the whole batch. In Step 2, for every segment, the input estimation (Section 4.1) is performed with the 5 selected  $\hat{\theta}_{B,I}$  vehicle parameters to form the  $\hat{n}_{rl/rr}$  compensated wheel rotation signals.

For the illustration of the effectiveness of model calibration, the parameter estimation is performed in 4 cases, for every segment separately with the pure G-N method (Section 3.1), and for all at once in the batch mode (Section 3.2), and both with the measured  $\tilde{n}_{rl/rr}$  and compensated  $\hat{n}_{rl/rr}$  inputs. The identified parameters can be found in the plots of Figure 7.

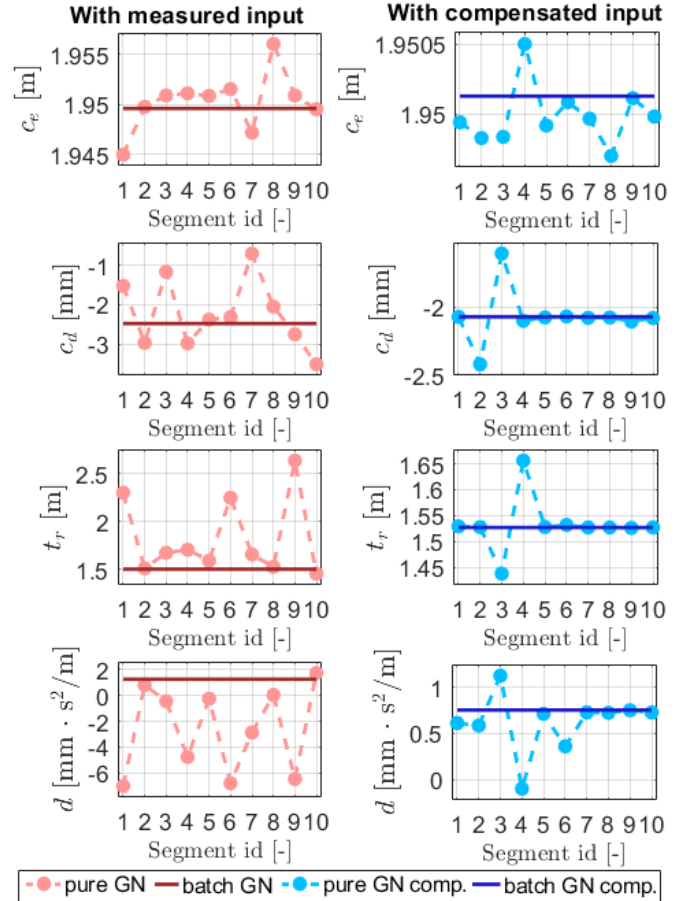


Fig. 7. Identified parameters with the  $\tilde{n}_{rl/rr}$  raw measured and the  $\hat{n}_{rl/rr}$  estimated wheel rotation signals. The final  $\hat{\theta}_{B,F}$  calibration of the proposed method is the batch GN comp. value.

The examined batch (id 34) is the worst of the 50 initial calibration which is illustrated well with the pure G-N calibrations when the measured inputs are utilized (left column of Figure 7). The estimated parameters differ from each other significantly, and in many cases, the values are incorrect, e.g. higher than 1.7  $m$  for  $t_r$  track width or negative  $d$  dynamic constant. The batch formulation of the G-N method reduces the distortion effects, the identified parameters are not incorrect (third row of Table 1). However, the 3.86  $m$  validation error (Figure 4) demonstrates that the bias of the calibration is still high.

When the compensated inputs are utilized in the calibrations (blue in Figure 7), the results are improved substantially. There are only two segments (3,4) in the case when the calibration is performed on the segments separately when the estimated parameters differ from the others significantly, but these are not incorrect values either.

The effectiveness of the input compensation is illustrated in Figure 8, where the validation errors of the pure and batch G-N estimations are presented. The outstanding result is that (regardless of the two mentioned segments), when the  $\hat{n}_{rl/rr}$  compensated inputs are utilized, the accuracy of model calibrations in the case of separate segments is far higher than the case of batch calibration with 10 segments all at once with the raw measured inputs.

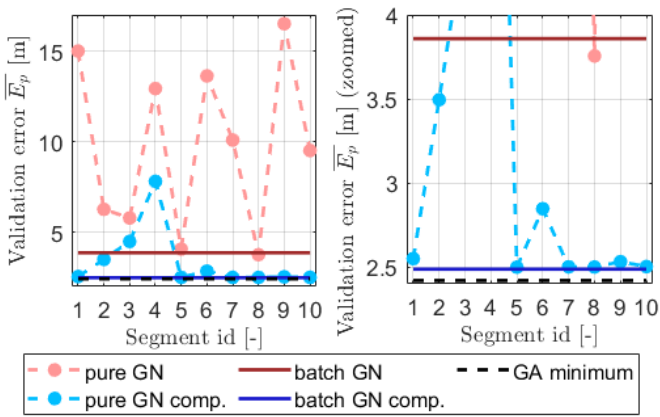


Fig. 8.  $\overline{E_p}$  average position error of the calibrated models

Furthermore, in the batch case with compensated inputs ( $\hat{\theta}_{B,F}$ ), the validation error is only 2.48 m which is only 8 cm higher than the reachable minimum error. In this paper, only the calibration of the examined batch 34 is shown in detail (since this is the worst of the initial calibrations), but the results are the same for the other batches as well.

### 6.5 Analysis of the estimation accuracy

The uncalibrated nominal setting from the vehicle’s datasheet ( $\theta_{nom} = [1.98, 0, 1.55, 0]^T$ ) is also tested. Its validation error is 11.09 m illustrating the requirement of the calibration. Taking into account that the minimum validation error is 2.40 m, thus the estimation accuracy with the proposed method compared to the case when the uncompensated inputs are utilized (3.86 m) is 18 times lower in a relative term. The 2.48 m average position error on 300 m long segments using only the wheel rotations is lower than 1% which corresponds to a highly accurate odometry-based localization.

## 7. CONCLUSION

In this paper, a complex calibration algorithm with a novel input compensation method was presented to the nonlinear wheel odometry model. The vehicle parameters are identified with the Gauss-Newton method, while the wheel rotation inputs are estimated as an optimal control task, and the methods are integrated into a 3 steps architecture. The main contribution is that an almost unbiased calibration can be obtained, even from a few 150 m long segments, if the wheel rotation input signals are compensated with the proposed algorithm.

In the future, we would like to improve the proposed method with the reduction of computation time to develop an online version of the method. The estimation of the segments can be done in parallel running, furthermore, we would like to examine in detail the relation between the utilized  $\hat{\theta}_{B,I}$  parameter values and the estimated input, to reduce the number of estimates required for the formation of the compensated input signals.

## REFERENCES

Antonelli, G. and et al. (2005). A calibration method for odometry of mobile robots based on the least-squares

technique. *IEEE Transactions on Robotics*, 21(5), 994–1004.

Bevly, D.M., Ryu, J., and Gerdes, J.C. (2006). Integrating ins sensors with gps measurements for continuous estimation of vehicle sideslip. *IEEE Transactions on Intelligent Transportation Systems*, 7(4), 483–493.

Brunker, A., Wohlgenuth, T., Frey, M., and Gauterin, F. (2017). GNSS-shortages-resistant and self-adaptive rear axle kinematic parameter estimator (SA-RAKPE). In *28th IEEE Intelligent Vehicles Symposium*.

Caron, F., Duflos, E., Pomorski, D., and Vanheeghe, P. (2006). GPS/IMU data fusion using multisensor Kalman-filtering: Introduction of contextual aspects. *Information Fusion*, 7(2), 221–230.

Censi, A., Franchi, A., Marchionni, L., and Oriolo, G. (2013). Simultaneous calibration of odometry and sensor parameters for mobile robots. *IEEE Transactions on Robotics*, 29(2), 475–492.

Fazekas, M., Gáspár, P., and Németh, B. (2021). Calibration and improvement of an odometry model with dynamic wheel and lateral dynamics integration. *Sensors*, 21(2).

Fazekas, M., Németh, B., Gáspár, P., and Sename, O. (2020). Vehicle odometry model identification considering dynamic load transfers. In *28th Mediterranean Conference on Control and Automation (MED)*, 19–24.

Funk, N., Alatur, N., and Deuber, R. (2017). Autonomous electric race car design. In *International Electric Vehicle Symposium*.

Jung, D., Seong, J., bae Moon, C., Jin, J., , and Chung, W. (2016). Accurate calibration of systematic errors for car-like mobile robots using experimental orientation errors. *International Journal of Precision Engineering and Manufacturing*, 17(9), 1113–1119.

Lemmer, L., Heb, R., Krauss, M., and Schilling, K. (2010). Calibration of a car-like mobile robot with a high-precision positioning system. In *2nd IFAC Symposium on Telematics Applications*.

Ljung, L. (1987). *System Identification*. PTR Prentice Hall.

Martinelli, A. and Siegwart, R. (2006). Observability properties and optimal trajectories for on-line odometry self-calibration. In *IEEE Conference on Decision and Control*, 3065–3070.

Mathworks (2021). Matlab optimization toolbox: quadprog. <https://www.mathworks.com/help/optim/ug/quadprog.html>.

Maye, J., Sommer, H., Agamennoni, G., Siegwart, R., and Furgale, P. (2016). Online self-calibration for robotic systems. *The International Journal of Robotics Research*, 35(4), 357–380.

Schoukens, J. and Ljung, L. (2019). Nonlinear system identification: A user-oriented roadmap. *IEEE Control Systems Magazine*, 39(6), 28–99.

Seegmiller, N., Rogers-Marcovitz, F., Miller, G., and Kelly, A. (2013). Vehicle model identification by integrated prediction error minimization. *The International Journal of Robotics Research*, 32(8).

Tangirala, A.K. (2015). *Principles of System Identification*. CRC.

Thrun, S. and et al. (2006). Stanley: The robot that won the DARPA Grand Challenge. *Journal of Field Robotics*, 23(9).